Incorporation of Carbon Nanotubes into Polyethylene by High Energy Ball Milling: Morphology and Physical Properties

GIULIANA GORRASI,[1] MARIA SARNO,[1] ANTONIO DI BARTOLOMEO,[2] DIANA SANNINO,[1] PAOLO CIAMBELLI,[1] VITTORIA VITTORIA[1]

[1]Department of Chemical and Food Engineering, University of Salerno, Via Ponte don Melillo, 84084 Fisciano (SA), Italy

[2]Department of Physics, University of Salerno, Via S. Allende, 84081 Baronissi (SA), Italy

Received 26 July 2006; revised 16 November 2006; accepted 18 November 2006
DOI: 10.1002/polb.21070
Published online in Wiley InterScience (www.interscience.wiley.com).

ABSTRACT: High energy ball milling (HEBM) was utilized, as an innovative process, to incorporate carbon nanotubes (CNTs) into a polyethylene (PE) matrix avoiding: high temperatures, solvents, ultrasonication, chemical modification of carbon nanotubes. Composites with 1, 2, 3, 5, and 10 wt % of carbon nanotubes were prepared. Films were obtained melting the powders in a hot press. Morphology and physical properties (thermal, mechanical, electrical properties) were evaluated. The used processing conditions allowed to obtain a satisfactory level of dispersion of CNTs into the PE matrix with a consequent improvement of the physical properties of the samples. The thermal degradation was significantly delayed already with 1–2% wt of CNTs. The mechanical properties resulted greatly improved for low filler content (up to 3% wt). The electrical measurements showed a percolation threshold in the range 1–3 wt % of CNTs. ©2007 Wiley Periodicals, Inc. J Polym Sci Part B: Polym Phys 45: 597–606, 2007
Keywords: nanocomposites; polyethylene (PE); thermal properties

INTRODUCTION

Carbon nanotubes (CNTs), since their discovery, have attracted the attention of researchers in various fields such as chemistry, physics, materials science, and electrical engineering. They are unique nanostructured materials with remarkable physical and mechanical properties,[1–5] such as high elastic modulus, as well as remarkable thermal and electrical conductivity, making them a very attractive candidate in composite material formulations. For this reason a current flurry of research is focused on the manufacturing of nanotube reinforced polymer matrix composites.[6–9] The main challenge is to transmit the excellent properties of CNTs to composites in which a polymer is the matrix, by combining the right choice of materials with the appropriate processing method.[10] To date, this research has focused on the following three main goals: (i) improvement of mechanical properties and performance, (ii) enhancement of thermal and flammability properties,[11–14] and (iii) of electrical conductivity.[15,16] CNTs have been proposed as conducting fillers to reduce the electrical resistivity of polymeric matrices for applications where static electrical dissipation is needed, such as in antistatic panels, protections or packages of electronic components, exterior automotive parts, and so forth.[7,16–21] Small amounts of carbon nanotubes can lower the resistivity of a polymer to values for which at least 10 times higher concentrations of traditional conductor fillers, such as carbon black or metallic powders, are needed.

Correspondence to: G. Gorrasi (E-mail: ggorrasi@unisa.it)
Journal of Polymer Science: Part B: Polymer Physics, Vol. 45, 597–606 (2007)

Consequently, CNTs offer the possibility of fabricating in a cost effective manner high performance polymers without impairing—indeed even enhancing—other polymeric properties.

To achieve the most effective enhancement of properties, the reinforcement phase must be uniformly dispersed in the matrix. However, carbon nanotubes are strongly affected by Van der Waal's forces, due to their small size and large surface area. These forces give rise to the formation of aggregates, which, in turn, make the dispersion of CNTs in polymers difficult. Overcoming this "clumping" of nanotubes is a critical issue in the fabrication of CNTs/polymer composites.[22,23] Currently there are three commonly used methods for incorporating carbon nanotubes into thermoplastic polymers:[17,24] *in situ* polymerization, solution method, and melt processing.

An alternative and innovative strategy relies on solid-state mixing at near room temperature, which ought to involve an efficient mixing of two or more species by mechanical milling, avoiding high temperatures and solvents. High Energy Ball Milling (HEBM) is an effective unconventional technique currently used in material synthesis and processing.[25] It consists of repeated events of energy transfer, promoted by the milling device, from the milling tools (generally balls) to the milled powder. During the milling, the powder particles crack, clean surfaces are produced, atom diffusion and "intimate mixing" are promoted.[25,26] As a consequence of the prolonged milling action, when the energy transferred during the hit is enough to overcome the activation barrier, chemical reactions may occur.

Recently it has been proved that HEBM on polymeric materials can help in obtaining materials with new characteristics, which can be barely achieved through other conventional processes.[27,28] HEBM of powders constituted by organic polymers and fillers has been proved to be an alternative and efficient technique to produce novel composites. This technique may support the more conventional and utilized techniques for producing nanocomposites, mainly based on *in situ* polymerization and melt extrusion.[29] In this paper, we report the preparation and the analysis of the morphology, as well as the physical properties of composites based on multi wall carbon nanotubes (MWNTs) dispersed in a linear low density polyethylene (LLDPE).

LLDPE is one of the most common polymers in several fields of technology, including nanotechnology. The addition of CNTs into the LLDPE matrix is expected to be a useful way to enhance its physical properties. In the present work, CNTs dispersion was performed through HEBM at room temperature, without any chemical modification or physical treatment of the CNTs. It is worth emphasizing that such technology, to date, has never been utilized for producing composites polymers/carbon nanotubes.

EXPERIMENTAL

Carbon Nanotubes Preparation

MWNTs have been synthesized by ethylene catalytic chemical vapor deposition (CCVD)[30–32] on Co/Fe-MgO catalyst, prepared by wet impregnation of MgO powder with cobalt acetate (2.5 wt %) and iron acetate (2.5 wt %) ethanol solution and drying at 140 °C for 12 h. Ethylene CCVD was carried out in a continuous flow reactor fed by ethylene-helium gas mixture. The reactor is a quartz tube (16 mm internal diameter, 300 mm length), a portion of which is filled with about 350 mg of catalyst. An external coaxial quartz tube (35 mm internal diameter) allows the reactant stream to be preheated. The temperature of catalyst bed is measured with a K thermocouple located inside a third coaxial quartz tube (4 mm internal diameter). The reactor is heated by an electrical oven, whose temperature is controlled by a temperature programmer-controller (Eurotherm 2408). Cylinder gases (99.9998 pure ethylene and 99.9990 pure helium) were mixed to give the ethylene/helium stream to feed the reactor. For each gas a mass flow controller (MFC) assured constant flow rate. The reactor temperature was increased from 25 °C up to 600 °C (5 °C/min) under helium flow and then 300 (stp) cm^3/min flow rate of 10% ethylene in helium was fed to the reactor. After 60 min, the ethylene–helium flow was stopped, the reactor was cooled to room temperature under helium flow, and a composite powder (carbon + catalyst) was recovered (MW1).

The as produced material, containing carbon nanotubes together with amorphous carbon, and catalyst was treated with 50 wt % HCl aqueous solution to dissolve the MgO support and the solid residue was washed with distilled water, centrifuged and finally dried at 353 K for 12 h, obtaining sample MW2. Carbon, so obtained, was then thermally treated to oxidize amorphous carbon and finally attached with HCl/HNO_3 to eliminate metal particles. High purity multiwalled carbon nanotubes (MW3) were obtained.

HEBM Procedure

Linear low density polyethylene (LLDPE) (Flexirene ® CM50) was supplied from Polimeri Europa (Italy) in ultrafine powder form, to promote the best mixing during the milling. Powders of MWNTs and polyethylene were milled in the solid state in a Retsch (Germany) centrifugal ball mill (model S 100). Samples mass were milled in a cylindrical steel jar of 50 cm^3 with 5 steel balls of 10 mm of diameter. Rotation speed used was 580 rpm and milling time was fixed at 45 min.

In these experimental conditions, five composites LLDPE/CNTs with 1, 2, 3, 5, and 10 wt % of carbon nanotubes were prepared. An LLDPE sample to be taken as a reference was also milled in absence of CNTs.

The LLDPE/CNTs mixtures and the pure milled LLDPE were molded in a hot press (Carver) at 200 °C, forming (250 ± 50) μm thick films, which were rapidly quenched in a water-ice bath (0 °C).

The samples will be coded as follows: PE (pure polymer), PENTX (polymer composite), where $X = 1, 2, 3, 5, 10$ is the weight percent of CNTs.

Methods

Field emission scanning electron microscopy (FESEM) pictures were obtained with a LEO 1525 microscope. The samples were covered with a 250 Å thick gold film using a sputter coater (Agar mod. 108 A).

Transmission electron microscopy (TEM) images were obtained with a Jeol 1200 EX2 microscope. The preparation of samples for TEM observation involved sonication in ethanol for 2–5 min and deposition of the sample on a carbon grid.

Thermogravimetrical analysis (TGA) was carried out with a Mettler TC-10 thermobalance. Polymer composites samples (~17 mg) were heated from 25 to 800 °C at 10 °C/min heating rate under air flow. The weight loss was recorded as a function of temperature.

The mechanical properties of the samples were evaluated from stress-strain curves obtained using a dynamometric apparatus INSTRON 4301. The measurements were carried out at room temperature on specimens cut from the films having thickness 0.1 mm and width 5 mm. The initial length of the samples between the clips machine was 10 mm. The deformation rate was 10 mm/min.

Differential scanning calorimetry (DSC) measurements were carried out using a thermal analyzer Mettler DSC 822/400 under N_2 atmosphere at a heating rate of 10 °C/min between −50 and 200 °C.

Raman spectra were obtained at room temperature with a microRaman spectrometer Renishaw in Via with 785 nm excitation wavelength (laser power 30 mW).

Electrical conductivity was measured with a Keithley 4200 SCS, which enables high accuracy DC measurements of I-V characteristics over a wide range (1.05pA–105mA; 210mV–210V).

Small strips of LLDPE/CNTs (~20 × 5 × 0.2 mm^3), with Pd/Pt sputter coated ends, were used as resistors between two dedicated holding clamps in a 2-probe resistance measurement set-up. Such a method was suitable for accurate measurements, since the resistance of the specimens is orders of magnitude higher than that of contacts and wires.

A DC voltage was applied along the length direction of the strips and the corresponding current was measured; to let the samples to adapt to the changing voltages (stepping from 0 to 100 V), a minimum delay of 180 s was kept between the application of the voltage and the measurement of the current. We checked that the alternative approach of forcing a current and measuring the voltage gave the same results.

Particular care was taken to avoid electrical disturbs and leakage currents. The LLDPE/CNTs strips were held in a shielded box (a Keithley 8006 text fixture). The connection to the 4200 SCS was realized through triax cables, with an intermediate and an external shield: the intermediate shield had the same voltage as the central signal wire to eliminate current leakages through the insulator; the external shield provided protection against electromagnetic disturbs.

Conductivity measurements were carried out at room temperature.

RESULTS AND DISCUSSION

Microscopy Observation

High purity MWNTs (>97%), after the purification steps, are obtained. MW3 TEM picture of Figure 1(a) gives clear evidence of the nanotubes' purity; typical impurities of the CCVD grown CNTs (such as amorphous carbon, and catalyst) are not observed, except for a few number of metal particles (black spots in the Figure). The tubes have an entangled structure, some helical are also visi-

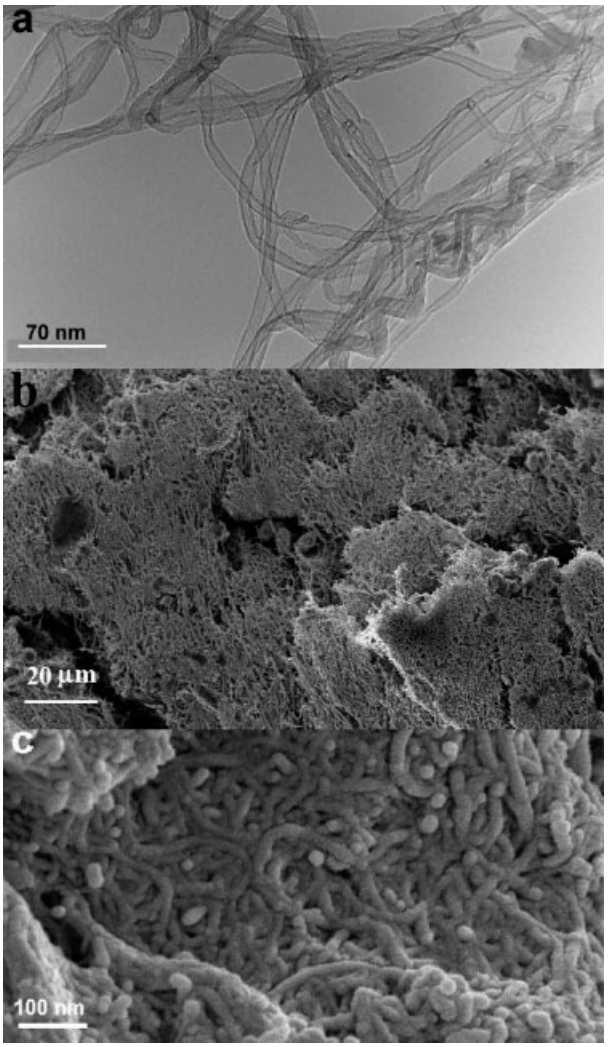

Figure 1. TEM image (a) and FESEM image (b,c) of sample MW3.

ble, permitting them to anchor better in the embedding matrix than straight nanotubes. The average diameter and length of the tubes are 10–15 nm and up to 10 μm respectively. FESEM image of purified carbon nanotubes [Fig. 1(b)] gives a clear picture of the tubes morphology with their bundle organization.

The morphology and the extent of dispersion of MWNTs in the polyethylene matrix were studied using a FESEM analysis. Pictures of the composite powders, after HEBM process, are shown in Figure 2. MWNTs can be clearly identified; they are uniformly dispersed as single nanotubes and as aggregates of few nanotubes and a good dispersion level can be observed for each sample.

FESEM pictures of carbon nanotubes recovered from sample PENT10 after thermal oxidation up to 505 °C are shown at two different

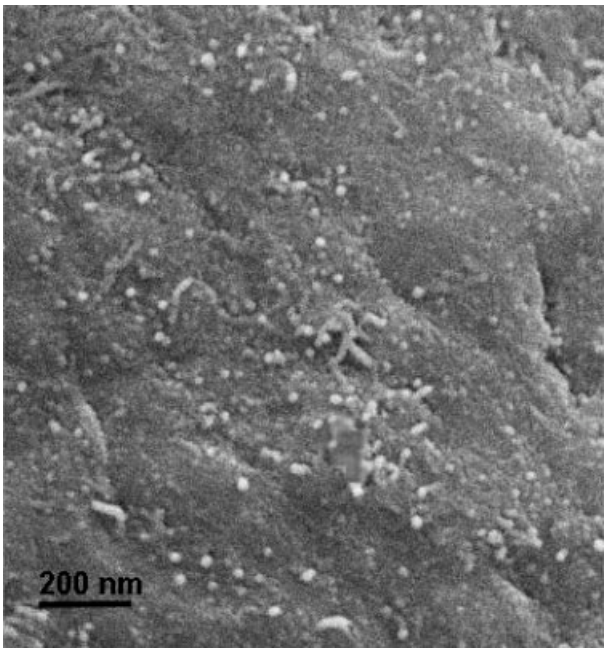

Figure 2. FESEM image of PENT3.

magnifications in Figure 3(a,b). It is evident that in the LLDPE-CNTs composite material, a loss of the original bundle organization occoccurred

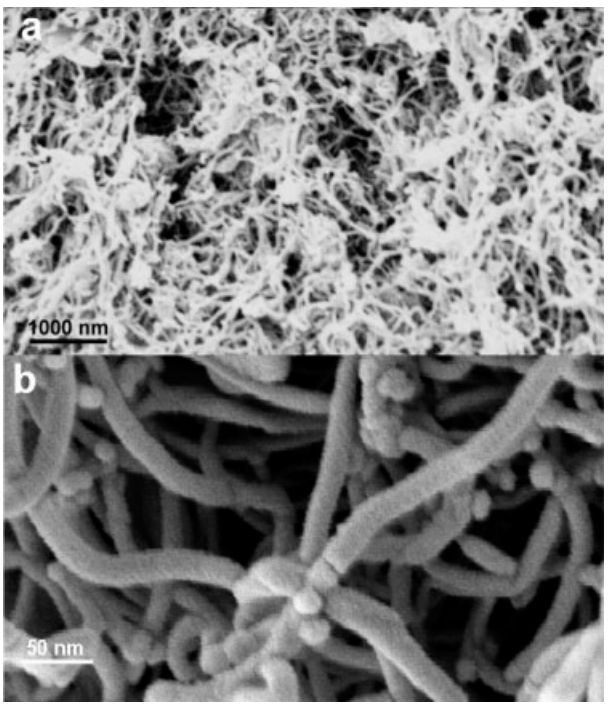

Figure 3. FESEM image at low resolution (a) and at high resolution (b) of sample recovered after thermal oxidation up to 505 °C of the polymer composites PENT10.

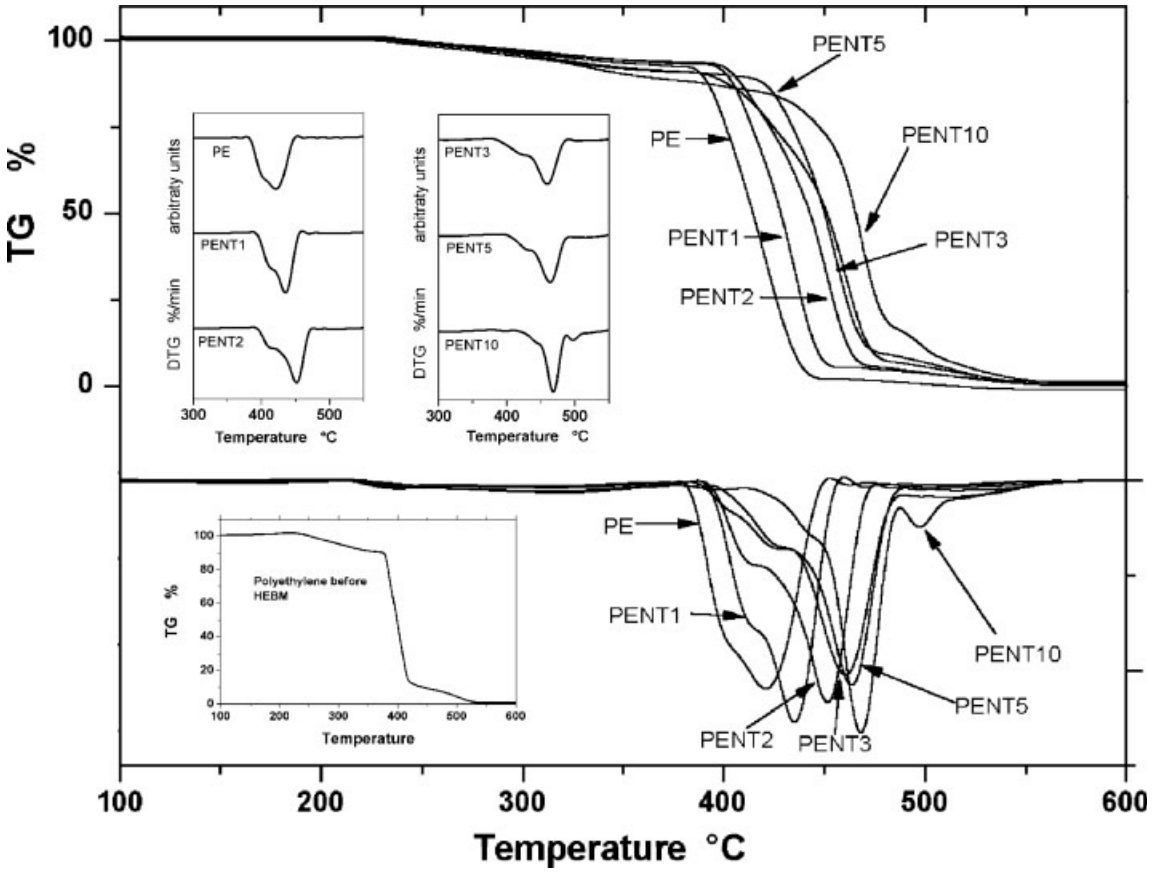

Figure 4. Air flow TG-DTG analysis in air of samples: PE, PENT1, PENT2, PENT3, PENT5, PENT10. The inset shows the DTG profiles in the range 300–550 °C.

[compare Figs. 1(b) and 3]. Carbon nanotubes appear well separated, indicating that the HEBM treatment, favoring carbon nanotubes disentangling, likely results in a good dispersion in the polymer matrix. From FESEM images, it is also possible to evaluate the tubes length after ball milling, which is about 4 μm.

TG-DTG Analysis

In Figure 4 air flow TG-DTG profiles of different PENT samples, in the range 100–600 °C are reported and compared with those of pure polyethylene. Figure 4 inset shows the DTG profiles in the range 300–550 °C. After a first small weight loss, all DTG profiles show a main peak with a lower temperature shoulder, and a final step relevant to CNTs and residual polymer fraction oxidation. The maxima position of two main DTG peaks, reported in Table 1, have been found by searching the minimum number of Lorentzians curves that fitted the different DTG profiles.

Pure milled PE shows an initial degradation temperature at about 221 °C. Above this temperature free radicals are generated leading to sequential degradation and breakdown of the main chain due to the thermal decomposition of the covalent C-C bond.[33] The two main PE oxidation stages, centered at 404 °C and 424 °C respectively, are to be ascribed to a two-step process, one of which controlled by the oxygen diffusion. In terms of solid state oxidation, the oxygen controlled step may be related to the oxidation of the bulk, while the first stage can be ascribed to the oxidation of the polymer surface and of the less ordered phase.[34] A small residue (~2%) oxidizes in a last step extending up to 550 °C. We have performed a thermogravimetrical measurement also on pure polyethylene, before milling (Fig. 4 bottom insert), that results practically close on that of PE after milling.

The incorporation of MWNTs in the polymer results in an increased oxidative stability of the composites. As a matter of fact, loading of 1 wt

Table 1. Effect of Carbon Nanotubes Loading Percentage on the Thermal Stability of the Composites

Sample	Main DTG Peaks Maxima (°C)		Mass Loss Ratio[a]
	1st	2nd	
PE	404	424	1.11
PENT1	415	435	1.15
PENT2	421	452	1.19
PENT3	424	459	1.71
PENT5	430	462	2.04
PENT10	442	468	3.45

[a] Mass loss ratio: mass loss in the 2nd oxidation stage/ mass loss before.

% of MWNTs determines an upshift of about 10 °C for both the two main DTG peaks maxima. On increasing the CNTs content we observe a progressive enhanced antioxidant effect (see Table 1), suggesting a good dispersion of the CNTs into the polymer.[13]

In Table 1, we also report the ratio between the mass loss in the 2nd oxidation stage and mass losses before, evaluated considering that they are proportional to the areas under DTG peaks. It is interesting to note that this ratio increases upon the MWNTs concentration increasing, indicating that the mass involved in the 2nd oxidation step depends on the MWNTs content in the composite. In addition, PENT10 shows a distinct 3rd oxidation step, centered at 500 °C, only pointed out at lower CNT concentration, probably due to carbon nanotubes nearest residual polymer fraction.

The increased oxidative stability of the composite materials can be explained either as an effect of the trap action exercised by CNTs on the polymer peroxyl radical, preventing their recombination,[13] or as a barrier effect to the oxygen diffusion or both. This second effect could partially explain the enhanced weight contribution to the observed second oxidation step. Further experiments are necessary to exhaustively explain the thermal and oxidative degradation behavior of the produced nanocomposite materials.

Thermal Properties

Thermal properties of the samples were investigated by means of DSC. Thermal data are reported in Table 2. The melting process of PE was clearly detected in the temperature range 120–150 °C, showing that the crystallization of the polymer chains was not inhibited by the nanotube content. In addition, considering the melting temperature of the pure PE (T_m = ~133 °C), we observed that the incorporation of the CNTs in the polymer did not cause a significant variation of T_m. The degree of crystallinity (X_c%) was evaluated using the simple formula: $(\Delta H_M/\Delta H_0)\times 100$, where ΔH_m (J/g) is the experimental enthalpy of fusion, and ΔH_0(J/g) is the enthalpy of fusion for a theoretically 100% crystalline PE, taken as 294 J/g.[34]

The degree of crystallinity results increased for incorporation of nanotubes, especially for 3% and 5% wt, while appears unmodified at higher percentages (i.e. 10% wt). This suggests a weak nucleating effect of the CNTs on the PE for low content.

Mechanical Properties

The enhancement of the mechanical properties of composites relies on two variables. (i) A high degree of load transfer between the matrix and the nanotubes is required. With a week interfacial adhesion between the phases, the nanotubes behave as holes or nanostructured flaws, introducing local stress concentrations, and the benefits of the CNTs properties are lost;[35] (ii) the nanotubes must be well dispersed. In case of poor dispersion, the nanotubes will fail by separation of the bundle rather than by failure of the nanotube itself, resulting in significantly reduced strength.[36–38]

The stress-strain curves of the samples, not reported, show the typical behavior of a semicrystalline system, which deforms with neck propagation. At the beginning, the stress is proportional to the deformation, according to Hook's law; after yield, there is an interval of almost constant stress, in which the neck, formed after the yield point, propagates to the whole sample. Following the neck propagation we observe a zone in which

Table 2. Thermal Properties of PE and PE/MWCNT Nanocomposites

Sample	T_m (°C)	X_c (%)[a]
PE	133	53
PENT1	132	54
PENT2	132	54
PENT3	133	57
PENT5	132	57
PENT10	133	53

[a] Normalized to PE content.

a higher stress is needed for small deformations, up to the breaking of the film. In this zone we are drawing an oriented fibrous structure, formed during the neck propagation step.

Figure 5 shows the mechanical parameters derived from the stress-strain curves. It is evident that small quantity of CNTs greatly improves the mechanical properties of the composites. In particular, the elastic modulus shows an increase of about 80% for composites with 1% and 2% of CNTs even if after milling the aspect ratio of nanotubes decreased. It is interesting to observe a significant increase of all the mechanical parameters of the polymer up to 3% of filler, and a plateau value at compositions over 3 wt %. The evolution of the composite crystalline fraction, evaluated by DSC, with the increase of CNTs content can meet to explain the nonlinear behavior of the composites mechanical properties with nanotubes content.[39,40] At low percentages there are two synergistic effects in improving the mechanical properties: CNTs and increasing of the crystallinity, at higher percentages the reinforcing effect is due only to the nanotubes content.

It is also worth noting that, at variance with many literature results on nanocomposites, the elongation at break point (ε_b%) does not decrease but is constant in all the investigated range of MWNTs concentration. Such results suggest a homogeneous network formed with the used processing conditions.

Raman Spectroscopy Analysis

Raman spectroscopy was used to investigate the interfacial interaction between the PE matrix and MWNT. Figure 6 shows the high frequency Raman spectra for PE and composites.

The spectrum of PE exhibits typical Raman modes of polyethylene. Carbon nanotubes show two main Raman lines, one at $\sim$1592 cm^{-1} (G line, due to the in-plane vibration of the C[sbond]C bonds), the other at $\sim$1320 cm^{-1} (D line, attributed to disorder induced by defects and curvature in the nanotube lattice and other carbon species).[41]

In the MWNTs/PE Raman spectra the characteristic bands of MWNTs are always easily identified (see in particular Fig. 6 inset), while those of PE become more and more weaker increasing nanotubes loading. However, the G line is shifted to higher wavenumbers, as reported for others nanocomposites with carbon nanotubes.[42] The shifting of the G band peak to higher frequencies can be explained by the disentangle-

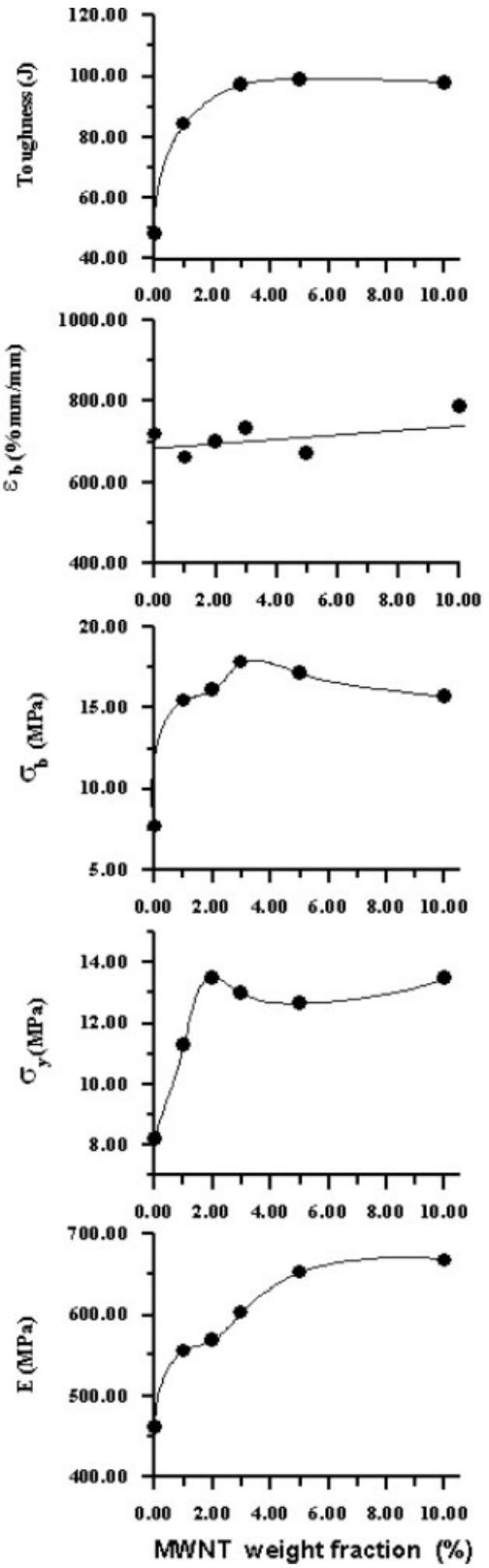

Figure 5. E (elastic modulus) [MPa], σ_y (stress at yield point) [MPa], σ_b (stress at break point) [MPa], ε_b (epsilon at break point) [mm/mm%], toughness [J] of LLDPE/CNTs composites as function of MWNT content.

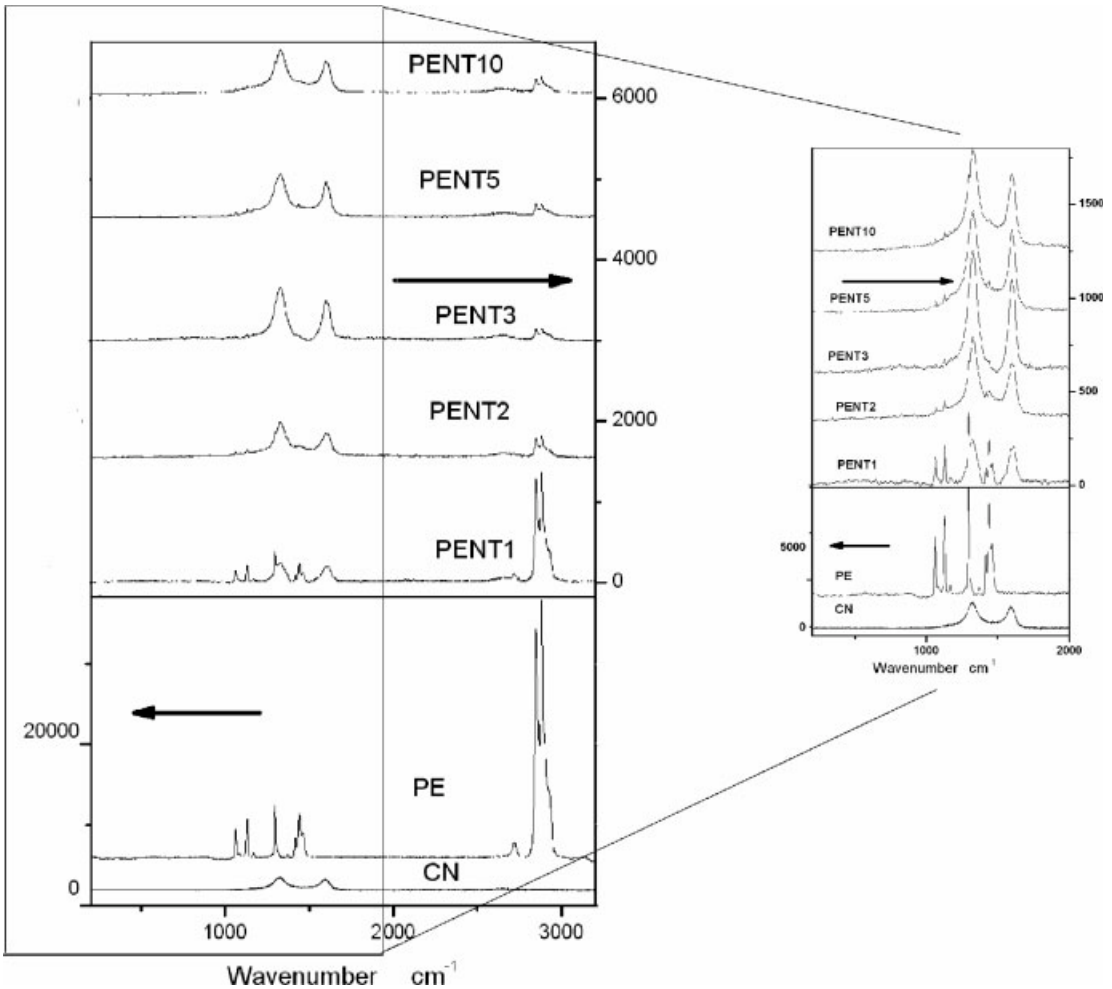

Figure 6. Raman spectra of PE, CN, and PENTs in the range 200–3200 cm^{-1}, in the inset are shown the spectra from 200 to 2000 cm^{-1}.

ment of the MWNT and subsequent dispersion in the PE matrix as a consequence of polymer penetration into the CNT bundles during the mixing.[39] The up-shifting of the D and G bands is also a consequence of strong compressive forces associated with PE chains on MWNT.

Electrical Properties

Electrical conductivity of carbon nanotubes filled polymers and its dependence on temperature, polymeric matrix, CNTs weight percentage and dispersion method have been extensively investigated.[16–20]

In this work, we focused on the study of the conductivity as a function of the CNTs weight content.

DC conductivity, which is shown in Figure 7 for increasing CNTs weight fractions, was extracted from I-V measurements around an applied voltage $V_{appl} = 50$ V, by using the basic formula

$$\sigma = \frac{L}{\tau W}\frac{1}{R} = \frac{L}{\tau W}\frac{I_{appl}}{V_{meas}}$$

where R, τ, W, and L are the resistance, the thickness, the width, and the length of the specimens respectively.

Since the I-V characteristics showed a nonlinear behavior, especially at low voltage; the value of 50 V was chosen being the I-V curves well fitted by a straight line around this voltage.

The value corresponding to the pure polymer results in values much higher than the average values of PE. Indeed, works on the conductivity of polyethylenes do not find a perfect agreement on the conductivity values.[43,44] The measurement of the current flowing through the polyethylene is difficult enough, because conduction current is

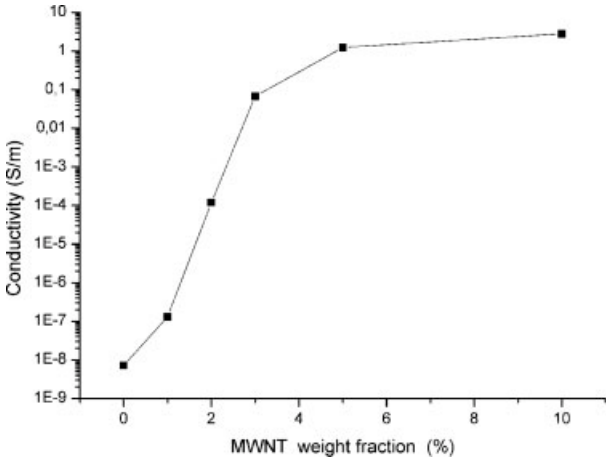

Figure 7. Electrical conductivity of LLDPE/CNTs composites as function of MWNT content.

very low, and spurious currents may appear owing to instabilities of the voltage source, environmental conditions, possible impurities of the polymer and/or catalytic residuals.

Between 1 and 3 CNTs wt %, the conductivity has a sizeable step of 6 orders of magnitude, a phenomenon that can be regarded as an electrical percolation with a percolation threshold around 2 wt %. It is worth noting that such results are in good agreement with others found for similar composites obtained by solution method[22] and significantly better than others obtained by melt blending for which the percolation threshold is at about 7.5% (wt/wt).[39]

According to the percolation theory, the conductivity s of a disordered mixture made of conducting (with volume fraction Φ) and insulating components should obey the law $\sigma = (\Phi - \Phi_c)^t$ for $\Phi \rightarrow \Phi_c^t$, where t is a parameter related to the dimensionality of the system and Φ_c is the percolation threshold. The stepwise change in conductivity is explained in terms of the formation of an interconnected tridimensional network of CNTs which provides a low resistance path to the moving charge carriers.

It is worthwhile noting that the conductivity values at 2 and 3 CNTs wt % are matched by PE matrices with 15–20 wt % of other conductive fillers.

CONCLUSIONS

High energy ball milling (HEBM) of powders constituted by polyethylene (PE) and multiwalled carbon nanotubes (MWNTs) has been proved to be an alternative and efficient technique to produce novel composites without using high temperatures, solvents and any physical and/or chemical treatment of the components. The improvement of thermal, mechanical, electrical properties of composites is very relevant for low nanotube content (2–3% wt).

REFERENCES AND NOTES

1. Iijima, S. Nature 1991, 354, 56–58.
2. Ajayan, P. M.; Zhou, O. Z.; Carbon Nanotubes: Synthesis, Structure, Properties, and Applications; Springer-Verlag: Berlin, 2000.
3. Saito, R.; Dresselhaus, G.; Dresselhaus, M. S. Physical Properties of Carbon Nanotubes;Imperial College Press: London, 1999.
4. Grimes, C. A.; Mungle, C.; Kouzoudis, D.; Fang, S.; Eklund, P. C. Chem Phys Lett 2000, 319, 460–464.
5. Files, B. S.; Mayeaux, B. M. Adv Mater Process 1999, 156, 47–49.
6. Kearns, J. C.; Shambaugh, R. L. J Appl Polym Sci 2002, 86, 2079–2084.
7. Safadi, B.; Andrews, R.; Grulke, E. A. J Appl Polym Sci 2002, 84, 2660–2669.
8. Wang, Y.; Cheng, R.; Liang, L.; Wang, Y. Compos Sci Technol 2005, 65, 793–797.
9. Tong, X.; Liu, C.; Cheng, H.; Zhao, H.; Yang, F.; Zhang, X. J Appl Polym Sci 2004, 92, 3697–3700.
10. Lordi, V.; Yao, N. J Mater Res 2000, 15, 2770–2779.
11. Celzard, A.; McRae, E.; Furdin, G.; Marêché, J. F. J Phys: Condens Matter 1997, 9, 2225–2229.
12. Sarno, M.; Gorrasi, G.; Sannino, D.; Sorrentino, A.; Vittoria, V.; Ciambelli, P. Macromol Rapid Commun 2004, 25 1963–1967.
13. Watts, P. C. P.; Fearon, P. K.; Hsu, W. K.; Billingham, N. C.; Kroto, H. W.; Walton, D. R. M. J Mater Chem 2003, 13, 491–495.
14. Kashiwagi, T.; Grulke, E.; Hilding, J.; Groth, K.; Harris, R.; Butler, K.; Shields, J.; Kharchenko, S.; Douglas, J. Polymer 2004, 45, 4227–4239.
15. Dufresne, A.; Paillet, M.; Putaux, J. L.; Canet, R.; Carmona, F.; Delhaes, P.; Cui, S. J Mater Sci 2002, 37, 3915–3923.
16. Sandler, J.; Shaffer, M. S. P.; Prasse, T.; Bauhofer, W.; Schulte, K.; Wind, A. H. Polymer 1999, 40, 5967–5971.
17. Potschke, P.; Formes, T. D.; Paul, D. R. Polymer 2002, 43, 3247–3255.
18. Andrews, R.; Jacques, D.; Minot, M.; Rantell, T. Macromol Mater Eng 2002, 287, 395–403.
19. Benoit, J. M.; Corraze, B.; Chauvet, O. Phys Rev B 2002, 65, 241405–241408.
20. He, X. J.; Du, J. H.; Ying, Z.; Cheng, H. M.; He, X. J Appl Phys Lett 2005, 86, 062112–062114.
21. Cashell, E. M.; Cohey, J. M. D.; Wardell, G. E.; Mc Brierty, V. J.; Douglass, D. C. J Appl Phys 1981, 52, 1542–1547.

22. Lau, K. T.; Hui, D. Carbon 2002, 40, 1605–1606.
23. Wood, J. R.; Zhao, Q.; Wagner, H. D. Compos A 2001, 32, 391–399.
24. Jin, Z.; Pramoda, K. P.; Goh, S. H.; Xu, G. Mater Res Bull 2002, 37, 2711–2715.
25. Suryanarayana, C. Prog Mater Sci 2001, 46, 1–184.
26. Gilman, P. S.; Benjamin, S. J. Annu Rev Mater Sci 1983, 13, 279–286.
27. Shaw, W. J. D. Mater Sci Forum 1998, 19, 269–272.
28. Padella, F.; Magini, M.; Incocciati, E. E. U. 2003–39 Patent No. 0963825, B1 Bulletin, 2003.
29. Sorrentino, A.; Gorrasi, G.; Tortora, M.; Vittoria, V.; Costantino, U.; Marmottini, F.; Padella, F. Polymer 2005, 46, 1601–1608.
30. Yacaman, M. J.; Yoshida, M. M.; Rendon, L.; Santiesteban, J. G. Appl Phys Lett 1993, 62, 202–204.
31. Ciambelli, P.; Sannino, D.; Sarno, M.; Fonseca, A.; Nagy, J. B. J Nanosci Nanotechnol 2004, 4, 779–787.
32. Ciambelli, P.; Sannino, D.; Sarno, M.; Fonseca, A.; Nagy, J. B. Carbon 2005, 43, 631–640.
33. Jana, R. N.; Mukunda, P. G.; Nando, G. B. Polym Degrad Stabil 2003, 80, 75–82.
34. Brandrup, J.; Immergut, E. H. Polymer Handbook;Wiley Interscience: New York, 1999.
35. Broska, R.; Rychly, J. Polym Degrad Stabil 2001, 72, 271–278.
36. Harmon, J. P.; Muisener, P. A. O.; Clayton, L.; D'Angelo, J.; Sikder, A. K.; Kumar, A.; Meyyaooan, M.; Cassell, A. M. In Surface Engineering 2001: Fundamentals and Applications (Materials Research Society Symposium Proceedings, Vol. 697); Materials Research Society: Boston, 2002; pp 425–435.
37. Bubert, H.; Haiber, S.; Brandl, W.; Marginean, G.; Heintze, M.; Bruse, V. Diamond Relat Mater 2003, 12, 811–817.
38. Schadler, L. S.; Giannaris, S. C.; Ajayan, P. M. Appl Phys Lett 1998, 73, 3842.
39. McNally, T.; Potschke, P.; Halley, P.; Murphy, M.; Martin, D.; Bell, S. E. J.; Brennan, G. P.; Bein, D.; Lemoine, P.; Quinn, J. P. Polymer 2005, 46, 8222–8232.
40. Cadek, M.; Coleman, J. N.; Barron, V.; Hedicke, K.; Blau, W. J Appl Phys Lett 2002, 81, 5123–5125.
41. Rao, A. M.; Richter, E.; Bandow, S.; Chase, B.; Eklund, P. C.; Williams, K. A.; Fang, S.; Subbaswamy, K. R.; Menon, M.; Thess, A.; Smalley, R. E.; Dresselhaus, G.; Dresselhaus, M. S. Science 1997, 275, 187–191.
42. McCarthy, B.; Coleman, J. N.; Czerw, R.; Dalton, A. B.; in het Panhuis, M.; Maiti, A.; Drury, A.; Bernier, P.; Nagy, J. B.; Lahr, B.; Byrne, H. J.; Carroll, D. L.; Blau, W. J. J Phys Chem B 2002, 106, 2210–2216.
43. Adamec, V.; Calderwood, J. H. J Phys D: Appl Phys 1981, 14, 1487.
44. Liang, G. D.; Tjong, S. C. Mater Chem Phys 2006, 100, 132–137.